

Accepted Manuscript

Title: Toward rational design of organic dye sensitized solar cells (DSSC): an application to the TA-St-CA dye

Authors: Narges Mohammadi, Peter J. Mahon, Feng Wang

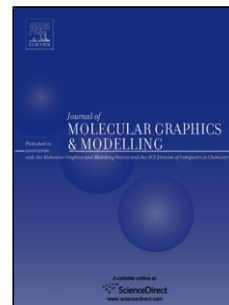
PII: S1093-3263(12)00148-9
DOI: doi:10.1016/j.jmgm.2012.12.005
Reference: JMG 6236

To appear in: *Journal of Molecular Graphics and Modelling*

Received date: 17-9-2012
Revised date: 18-12-2012
Accepted date: 19-12-2012

Please cite this article as: N. Mohammadi, P.J. Mahon, F. Wang, Toward rational design of organic dye sensitized solar cells (DSSC): an application to the TA-St-CA dye, *Journal of Molecular Graphics and Modelling* (2010), doi:10.1016/j.jmgm.2012.12.005

This is a PDF file of an unedited manuscript that has been accepted for publication. As a service to our customers we are providing this early version of the manuscript. The manuscript will undergo copyediting, typesetting, and review of the resulting proof before it is published in its final form. Please note that during the production process errors may be discovered which could affect the content, and all legal disclaimers that apply to the journal pertain.



Toward rational design of organic dye sensitized solar cells (DSSC): an application to the TA-St-CA dye

Narges Mohammadi, Peter J. Mahon and Feng Wang*

eChemistry Laboratory, Faculty of Life and Social Sciences, Swinburne University of Technology, Hawthorn, Melbourne, Victoria, 3122, Australia

- A rational design strategy through chemical modifications is developed to improve dye sensitizers used in solar cells, with applications to the TA-St-CA dye;
- Electron-donating (ED) and withdrawing (EW) units based on Dewar's rules are substituted to enhance the functionalities of new dyes; the positions of such substitutions are also suggested;
- The enhancement of the functionalities of the new dyes differs for the ED and EW substituted dyes without the same mechanisms;
- The three dimensional (3D) structure of the reference dye, TA-St-CA, are presented using an animated 3D-pdf file to achieve better spatial understanding of the dye. This 3D-pdf technique was recently developed by the group.

Toward rational design of organic dye sensitized solar cells (DSSC): an application to the TA-St-CA dye

Narges Mohammadi, Peter J. Mahon and Feng Wang*

eChemistry Laboratory, Faculty of Life and Social Sciences, Swinburne University of Technology, Hawthorn, Melbourne, Victoria, 3122, Australia

* Corresponding author. Tel.: +61 3 9214 5065; fax: +61-3-9214-5921.

E-mail addresses: fwang@swin.edu.au (F. Wang).

Abstract

A computer aided rational design has been performed on TA-St-CA dye sensitizer in order to improve the desirable properties for new organic dye sensitized solar cell (DSSC). A number of electron-donating (ED) and electron-withdrawing (EW) units based on Dewar's rules are substituted into the π -conjugated oligo-phenylenevinylene bridge of the reference TA-St-CA dye. The effects of these alternations on the molecular structures and the electron absorption spectra are calculated using time-dependant density functional theory (TDDFT). It is found that chemical modifications using electron donating (ED) substitutions exhibit advantages over the electron withdrawing (EW) substitutes to reduce the HOMO-LUMO energy gap as well as the electron distribution of the frontier orbitals of the new dyes. Dewar's rule is a useful guideline for rational design of new dye sensitizers with desired HOMO-LUMO gap. The impact on the optical spectra of new dyes are, however, less significant.

Keywords: rational dye design; DSSC; HOMO-LUMO gap; DFT calculations; Organic dye; Dewar's rule;

1. Introduction

Organic dye sensitized solar cells (DSSC) [1] as a new type of photovoltaic device are currently under extensive research as an inexpensive alternative to the most conventional expensive silicon-based devices. Over a thousand papers were published on DSSC just in 2010 [2]. As a key component of DSSC, the role of the adsorbed dye sensitizer is to excite electrons into excited states through absorbing visible and near infrared (NIR) solar radiation. Consequently these excited electrons will be injected to the conduction band of the nearest semiconductor.

Ruthenium-based dyes such as N3 [3, 4], N719 [4-6] and Black dye [7-9] are the best performing sensitizers for DSSC in terms of their stability and their efficiency in converting solar energy into electricity, able to exceed 11% under standard test conditions [4, 5]. However, these compounds contain ruthenium which is a rare and expensive metal whereas the preparation of organic dyes should be more cost effective in comparison. In addition, organic dyes have high absorption coefficients and tuneable optical properties [10-14]. The most important issue that organic dyes need to address is to improve their narrower absorbance spectrum which is less than Ru-based complexes [14, 15].

Dye sensitizer design is usually based on synthesis which is time consuming and expensive [14]. As a result, computer aided rational design of organic dye sensitizers has been very attractive and is becoming state-of-art, as *in silico* dye design based on the modification of existing dyes has become possible by exploiting high performance computing facilities paired with advanced and more accurate theoretical methods [16-21]. The present study is to improve the desirable properties of organic dye sensitizers

through rational substitutions on existing dyes based on Dewar's rule [22], using high performance computers. Computer aided study enables us to predict the properties of new dyes beforehand in order to identify the most appropriate new dyes. Such a rational design has been widely adopted in drug development [23-25].

The ideal sensitizer should have several characteristics. It should absorb all light below a threshold wavelength of about 920 nm (i.e. visible and near infra-red spectrum) [13, 15, 26]. By now, no dye has been found that injects in the whole visible and the NIR (Near Infra-Red) with the same efficiency. Most of the well-performing dyes such as N3 ruthenium-based dye lack the absorption in the NIR region (e.g. 750-900 nm for N3 dye). The short-circuit current density, J_{sc} , can be increased by extending the absorption region of dye sensitizer into NIR. This will increase the overall solar conversion efficiency, η , which is calculated according to the following formula:

$$\eta = \frac{V_{oc} J_{sc} FF}{P_{in}} \quad (1)$$

Where V_{oc} is the open-circuit voltage, FF is fill factor and P_{in} is the total solar power incident on the cell. Refer to [27] for comprehensive review of improving efficiency based on the above formula for DSSC.

For the stability of adsorption, dye sensitizer must also carry attachment groups such as carboxylate or phosphonate to firmly graft it to the semiconductor oxide surface [13, 28]. To produce a photocurrent density, the energy of the dye excited-state (manifested as the energy of LUMO) necessarily must be higher than the conduction band edge of the n-type semiconductor (e.g. TiO_2). High quantum efficiency for injection is achieved when the LUMO of the dye is both energetically matched and

reasonably strongly coupled to the underlying semiconductor [5-7]. In order to be rapidly regenerated via donation of electrons from a redox shuttle or hole-conductor, the HOMO of the dye sensitizer should lie below the energy level of the redox shuttle [3-5, 8, 9]. The dye should not have significant degradation in at least 20 years (10^8 turnover cycles) of operation and should sustain natural light for this period of time. In other words, it should satisfy long term stability [5].

It is known that modification of the conjugated bridge can shift the absorption spectrum in a push-pull dye [29]. A bathochromic (i.e. to a longer wavelength) shift, also known as red-shift, can enhance the overall efficiency of DSSC [30]. Perturbational molecular orbital theory (e.g. Dewar's rules [22]) can predict the effects of such alternations of the conjugation bridge. According to Dewar's rule, atoms on the π -conjugated bridge in a chromophore with "Donor, π -conjugated bridge, Acceptor" structure (D- π -A), can alternately be indexed as "starred" and "unstarred". According to perturbational molecular orbital theory, substituting electron donating groups on the starred positions results in an increase in the energy of highest occupied molecular orbital (HOMO). Substituting an EW group on unstarred positions in the bridge is expected to decrease the energy of the lowest unoccupied molecular orbital (LUMO). Both of these substitutions decrease the ΔE between HOMO and LUMO and cause a bathochromic shift [31].

2. Methods and computational details

A highly efficient organic dye sensitizer containing a π -conjugated oligophenylenevinylene bridge with electron donor-acceptor moieties (TA-St-CA) was designed and synthesized by Suyoung *et al.* [32] and achieves an overall solar-to-

energy conversion efficiency of 9.1%. This efficiency is very high for an organic sensitizer. As a result, we selected this push-pull dye as the conjugation backbone structure for all of the π -bridge modifications with the experimentally tested organic-dye sensitizer TA-St-CA dye employed as the backbone reference in the present study. Based on Dewar's rule as a guideline in this study and starting from the first position on the π -conjugated bridge of TA-St-CA dye, carbon atoms are labelled as starred and unstarred alternately as shown in Figure 1. Note that no substitution is possible on position 3 and 6* because there is no hydrogen atom available on these 2 positions. Perturbational molecular orbital theory (e.g. Dewar's rules [22]) serves as an indicator for the positions (starred or unstarred) and substituents (electron donating/withdrawing) on the π -conjugated bridge of the dye, to shift the spectral bands, and to change the energies of the highest occupied molecular orbital (HOMO) and the lowest unoccupied molecular orbital (LUMO) of the new dyes. A schematic description of Dewar's rule is illustrated in Figure 1 in supplementary information.

To improve the original TA-St-CA dye, it is required to redshift (bathochromic shift) the absorption spectrum and to reduce the HOMO-LUMO energy gap (ΔE) of the new dye. Based on Dewar's rule (i.e., perturbational molecular orbital theory), to move up the energy of the HOMO, an electron donating group (ED) needs to substitute on the starred positions of the π -conjugated bridge to form a new dye. Alternatively, to move down the energy of the LUMO, an electron withdrawing group (EW) needs to substitute on the unstarred positions of the π -conjugated bridge to form a new dye. Therefore, the new dyes can be rationally designed by replacing an ED group on the starred positions or an EW group on one of the unstarred positions of the π -conjugated bridge of the original dye, in order to result in desired properties of the new dyes [31].

Following Dewar's rule as a guideline, the present study designed new dye structures through the modifications on the π -conjugated bridge of the original TA-St-CA dye using various schemes and ED and EW groups listed in Table 1. For complete structures, refer to Table S1 in supplementary information.

All *ab initio* calculations are performed quantum mechanically, using density functional theory (DFT) based PBE0 hybrid density functionals [33] and polarized split-valence triple-zeta 6-311G(d) basis set, without any constraints. The DFT based PBE0 functional (a hybrid of PBE with 25% HF exchange term contribution) is found to be a reliable functional to estimate the excitation energies [34, 35]. It has been widely employed to study the colours of most industrial organic dyes. In an assessment on a set of more than 100 organic dyes for reproducing the experimental UV-Vis $\pi \rightarrow \pi^*$ absorption wavelength, it outperformed all other functionals of the study [36]. Therefore, the PBE0 functional has been proven a reliable functional to study the absorption spectra and molecular structures of organic dye sensitizers and we exploit this functional for this study. All calculations are based on Gaussian09 computational chemistry package [37].

The optimized geometry of the TA-St-CA dye was obtained in this study and to verify that the optimized structure is a true minimum, frequency calculations were performed on the optimized geometry and no imaginary frequencies were found on the optimized structure. Figure 1 presents the chemical structure of the TA-St-CA dye indicating the three important functional regions. The chemical structure of the reference TA-St-CA dye is also linked with the fully optimized structure in three-dimensional (3D) space using the 3D-pdf technique [38], a recently developed tool in

the research group. Double click on the TA-St-CA dye structure will activate the 3D-pdf function and use the mouse to move the structure for a better understanding of the TA-St-CA structure in 3D space on a computer.

The experimental UV–Vis spectrum of the original TA-St-CA dye was measured in ethanol solution [32]. In order to make comparisons, the present study simulated spectra of the reference TA-St-CA and the new dyes in ethanol solution using the conductor-like polarizable continuum model (CPCM) [39, 40].

For each substitution, the geometries of the new dyes are optimized followed by frequency calculations to ensure the structures are true minimal energy structures. The UV-Vis spectra in vacuum and in ethanol solution were calculated using singlet-singlet transitions up to lowest 30 spin-allowed excited states of each dye based on TDDFT calculations. A full width at half-maximum (fwhm) 2500 cm^{-1} (4000 nm) of the Gaussian curves is used to convolute the spectrum reported in this study. Single point calculations on the optimized structures in vacuum using the same computational model were employed to construct the molecular energy levels and isodensity plots.

3. Results and discussion

Figure 1 gives the optimized structure of the original TA-St-CA dye. It is composed of three moieties, an electron rich “triphenylamine” group acting as electron donor (D-section), an “oligo-phenylenevinylene” group and a “cyanoacrylic acid” group which works as electron acceptor/anchoring (A-section). Between the D-section and the A-section, there is a π -conjugated bridge (π -Bridge section) which connects the

electron donor and acceptor moieties to conduct the excited electrons of the dye sensitizer. In Figure 1, the A-section contains a carboxyl group as an anchoring unit to attach the dye onto TiO₂ semiconductor [32]. The four benzene rings in the molecular structure of the TA-St-CA dye are labelled as R₁-R₄ as seen in Figure 1.

Table 2 summarizes related properties such as geometric, dipole moments, and the π -conjugated bridge lengths which are the direct distances between C₍₁₈₎ and C₍₂₃₎ of the original and the new dyes. The optimized structure of TA-St-CA dye in the ground electronic state indicates that the π -conjugated oligo-phenylenevinylene bridge is almost planar, which is nearly coplanar with the cyanoacrylic acid group. Such a coplanar structure leads to the conjugation effects. Chemically modifying the conjugation bridge of the TA-St-CA dye produces a number of new dyes (structures *ED-I* to *EW-III* in Table1) which slightly deviate from the planarity. The four benzene rings in the molecular structure of the TA-St-CA dye are labeled as R₁-R₄ as seen in Figure 1. Perimeters of the terminal benzene rings R₃ and R₄ are slightly longer than the benzene rings inside the molecule, i.e., R₁ and R₂. For example, R₃ and R₄ are given by 8.38 and 8.37 Å, respectively, whereas both R₁ and R₂ are the same at 8.35 Å, which is the same as an isolated benzene ring [41]. For the TA-St-CA dye, this π -conjugated bridge length is calculated as 5.23 Å. In this table, substitutions of the EW group (i.e. CN) on 1, 5, and 7 positions of the π -conjugated bridge (i.e. structures *EW-I* to *EW-III* in last three columns of Table 2) extend the π -conjugated bridge length of the new dyes compared to the reference dye. The influence of the electron donating substitutions (EDS) is not as systematic with either shorter or longer distances apparent. However, it is noted that the “*ED-I*” and “*ED-IV*” new dyes possess the shortest π -conjugated bridge lengths of 5.13 and 5.10 Å, respectively, in this table. All

new dyes except for “*ED-I*” have a larger molecular size than the size of the reference dye with the electric extent ($\langle R^2 \rangle$) of 34612.20 a.u.

The dipole moments (μ) of the dyes exhibit a similar trend to the π -conjugated bridge length in general. That is, the substitutions of the EW group polarize the molecules and therefore produce a larger than the reference (6.58 Debye) dipole moment. For example, the new dyes of “*EW-I*”, “*EW-II*” and “*EW-III*” result in a noticeable increase in dipole moment of 8.38, 8.41 and 8.81 Debye, respectively. However, EDS reduce the dipole moment from the reference dye with the new dyes “*ED-I*” and “*ED-IV*” possessing smaller dipole moments of 4.63 and 4.64 Debye, respectively.

UV-Visible spectroscopy is the most appropriate technique to indicate the presence of chromophores in a molecule. Chromophores are π -electrons or electron lone pairs in a molecule which are likely to absorb light in the UV-Vis region (200 to 800 nm). As a result, conjugated π -electrons in a molecule becomes the major structural feature identified by this UV-Vis spectroscopic technique. The UV-Vis spectra of the new dyes given in Table 1 are displayed in Figure 2, which correlates the impact of the chemical structural modifications on the reference TA-St-CA dye with respect to their spectra. Figure 2 (a₁) compares the simulated UV-Vis spectra of the reference TA-St-CA dye in ethanol solution and in gas-phase with available experiment (in ethanol solution) [32]. It is seen that the calculated spectra agree reasonably well with the experiment which is only measured in the region of $\lambda < 450$ nm, i.e., the first absorption spectral peak region. The simulated UV-Vis spectrum of the reference TA-St-CA dye in ethanol solution closely reproduce the major spectral peak at $\lambda_{\text{I}} = 374.52$ nm with respect to the

experiment at $\lambda_I = 386$ nm (I). In the spectral region of $\lambda > 450$ nm, the present simulation in ethanol produces a major peak at $\lambda_{II} = 545.03$ nm in the green region (II), which is in agreement with an early computational study [42]. In addition, it is observed that the ethanol solvent causes the simulated spectral peaks of the reference dye to red-shift from their positions in vacuum. The good agreement with experiment and literature indicates that the present computational model employed is a good model.

It is found from the simulated spectra of the original dye that the most intensive absorption band observed at $\lambda_{II} = 545.03$ nm ($f = 1.2179$) corresponds to a transition (excitation) from the HOMO to the LUMO of the reference dye. As the HOMO-LUMO gap requires the least energy to excite an electron from an occupied orbital onto a virtual (unoccupied) orbital, there is no doubt that the HOMO-LUMO transition is almost always the favourite transition in energy. The second strongest absorption band near $\lambda_I = 374$ nm ($f = 0.773$) is a combination of two major transitions. One is dominated by the transition from HOMO-1 to LUMO (~91%) and the other is a minor transition from HOMO to LUMO+1 (~7%). The HOMO-1 \rightarrow LUMO and/or HOMO \rightarrow LUMO+1 transitions are usually the second energetically favourite transitions.

Figure 2(a₂) and (a₃) compare the simulated spectra of the new dyes obtained from electron donating substitutions with the original dye in ethanol solution, whereas Figure 2(a₄) compares the new dyes obtained from electron withdrawing substitutions with the original dye. Modifications of the reference dye results in shifts of the spectral peaks, either bathochromic shift (i.e. to the longer wavelength) or

hypsochromic shift (i.e. to the shorter wavelength) from positions of the reference dye. Chemical modifications by EDS with respect to the reference dye lead to bathochromic shift of peak II but hypsochromic shift of peak I in the new dyes *ED-I* to *ED-VI* and the EW groups result in bathochromic shift in both peak I and II in new dyes *EW-I* to *EW-III*. For example, the $-NH_2$ (EDS) group on the 2* position of the reference dye (produce a new dye “*ED-I*”) results in a bathochromic shift of ~44 nm on peak II, whereas a ~31 nm hypsochromic shift on peak I of the TA-St-CA spectrum (in ethanol solution). These results can be rationalised by looking at the underlying electronic transition orbitals. As discussed earlier, peak II is mainly (i.e. 99%) a HOMO→LUMO transition which are brought closer to each other in new dye “*ED-I*”; therefore, this peak is red-shifted in “*ED-I*” compared to TA-St-CA dye. On the other hand, an excitation transition from HOMO-1→LUMO ($\Delta E=3.76$ eV) is mainly (i.e. 91%) responsible for peak I in TA-St-CA structure, while a HOMO→LUMO+1 ($\Delta E=4.29$ eV) excitation contributes 90% to this peak in “*ED-I*”. It is seen that the first peak (I) in “*ED-I*” needs more energy compared to that of TA-St-CA dye because of its bigger energy gap and therefore it is shifted to longer wavelengths. Similar justification and reasoning hold for all other substitutions.

The width of the absorption bands and the absorption threshold of the main band (i.e. peak II) are the other two important factors in determining a more efficient dye [19]. The width of the main absorption band is slightly changed for all of the new dyes except for the new “*ED-VI*” dye (Refer to Table 3), but as seen in Figure 2 (a_2 , a_3 and a_4), these changes are not very significant. However, the influence of modifications on the maximum position of the main band (i.e. peak II) and the absorption threshold is

more apparent. For chemical modifications by EDS, the maximum position of the main band and the absorption threshold of “*ED-I*” and “*ED-IV*” are more red-shifted compared to those of the TA-St-CA dye, however, absorption is less strong in these two molecules compared to TA-St-CA dye (Refer to Table S3 in supplementary information). The new dye “*ED-II*” shows almost identical main peak (II) to that of TA-ST-CA dye. For “*ED-III*”, “*ED-V*” and “*ED-VI*” the maximum position of the main band and the absorption threshold of the main peak (II) is slightly red-shifted compared to TA-St-CA. Clearly, chemical modifications by EWS resulted in red-shift of both the position and the threshold of the main peak.

It should be noted that for a more precise study of the absorption spectra, the influence of the dye adsorption onto TiO₂ nanocrystals should also be taken into account. A number of TDDFT calculations on the dyes adsorbed onto TiO₂ have been reported [20, 43-47]. Although such calculations are beyond the scope of the current study, it is important to have a glimpse of the effect of adsorption on the electronic structure and absorption spectra of dye-TiO₂ system. In addition to altering the conduction band of the semiconductor [48], adsorption of dye sensitizer onto TiO₂ will change the electronic properties and absorption spectra of dye sensitizer. For example, it can change the stabilization of the LUMO of the dye sensitizer, leading to a red-shift of the absorption spectra of adsorbed dye compared to isolated dye. Sánchez-de-Armas *et al.* studied the optical properties of five coumarin-based dyes and observed a widening of the first band and small bathochromic shift in the absorption spectra of adsorbed coumarin dyes compared to free dye molecules[49]. Another study by Wen *et al.* shows that morphology and size of TiO₂ nanocrystals can influence the UV-Vis spectra of N17 sensitizer [50]. Another example is the

absorption spectra of free and bounded (onto TiO_2) catechol and alizarin molecules. Although these two molecules have similar binding patterns, upon binding onto TiO_2 an entirely new band is observed in the absorption spectra along with exactly the same bands of the free catechol spectra, whereas no new band appears and only red-shifting is observed for alizarin bound onto TiO_2 semiconductor [51]. In this study we only compared the absorption spectra of free dye molecules.

Figure 3 provides the molecular orbital (MO) energy diagrams of the TA-St-CA dye and the new dyes in vacuum, focusing on the HOMO-LUMO energy, as the spectra in Figure 2 are dominated by HOMO-LUMO transitions. As seen in Figure 3, the LUMO energies of all dyes are well located above the conduction band of the semiconductor, therefore enough energy force is provided for electron injection. It is also observed that the HOMO energy of all dyes is located below the energy level of iodide/triiodide for efficient regeneration of the oxidized dye. The orbital energies of the HOMO and the LUMO of the original TA-St-CA dye in vacuum are calculated at -5.51 and -2.69 eV, respectively, and their corresponding energy gap between HOMO and LUMO is given by 2.82 eV. In general, the EDS (i.e. on the 2*, 4* and 8* positions) lead to a decrease of the HOMO-LUMO gap but also lift up the of LUMO energy levels, as shown in the figure as structures *ED-I*, *ED-II*, *ED-III* ..., *ED-VI*. Only a few substitutions (such as on the 2* position of new dye *ED-I*) reduce the HOMO-LUMO gap by lifting up the HOMO energies without apparently lifting up the LUMO energies. Although the EW substitutions (on position 5 such as new dyes *EW-I*, *EW-II* and *EW-III*) of the reference dye result in the decrease of the HOMO-LUMO energy gap, too, the EW substitutions shift the energies of both the HOMO as well as the LUMO down. As can be predicted by the Dewar's rule [22, 31, 52], the

EW substitutions results in a decrease of HOMO-LUMO gap with larger energy drops of the LUMOs than the energy drops in the HOMOs. Reducing or increasing orbital energies of both LUMOs and HOMOs is not desirable if it results in an increase of the band gap. Alignment of LUMO energy level above the conduction band edge of semiconductor (i.e. TiO_2) and HOMO energy level under the redox potential of redox couple (i.e. Iodide/Triiodide) should also be considered in deciding about the suitability of the newly designed dyes. It is also known that electron injection rate would be increased by electron injection over-potential [53]. As a result, Figure 3 suggests that to reduce the HOMO-LUMO gap of a dye, the substitutions with an ED group on positions close to the D-section of the reference dye is a more appropriate approach to rational design of new dyes.

Table 3 collects the effects of chemical substitutions on a number of important properties of organic dyes, such as the energies of the HOMOs (ϵ_{HOMO}), the LUMOs (ϵ_{LUMO}), the HOMO-LUMO energy gap ($\Delta\epsilon$), shift of the spectral peaks ($\Delta\lambda_{\text{I}}$ and $\Delta\lambda_{\text{II}}$) as well as changes in their spectral widths ($\Delta\gamma$). In this table, the preferred property changes of the new dyes against the reference dye are in black, whereas the unfavourable changes are coloured in red. From this table, it is apparent that the new dye “ED-I” almost meets all the requirements of the preferred properties of an improved dye, except for the slight decrease in the wavelength of its first absorption peak (Refer to Table S1 and S2 in supplementary for more information). Although the EW substituted dyes, EW-I to EW-III, enable the bathochromic shift of the UV-Vis spectra from the reference dye, they hardly meet the other requirements for functionally enhanced dyes.

To further explore the different behaviours of the ED and EW impact on the reference (TA-St-CA) dye, Figure 4 provides the information of the HOMOs and the LUMOs of the reference (TA-St-CA) dye, the new dyes produced by an EDS (new dye “*ED-I*”) and an EWS (new dye “*EW-I*”). As seen from this figure, the HOMO of TA-St-CA is a π orbital (dominated by p electrons from the backbone atoms) and populates over the entire triphenylamine donor group (R_2 , R_3 and R_4 , refer to D section of the D- π -A dye in Figure 1) and partially populates the oligo-phenylenevinylene π -conjugated bridge and the R_1 ring, as shown in the box in this figure. The LUMO is a singlet π^* orbital which largely populates the cyanoacrylic acid acceptor group (the A section of the D- π -A dye). The LUMO also spreads into the π -conjugated bridge and into the triphenylamine donor group of R_2 ring in the D-section. As a result, the HOMO to LUMO transition ensures the intra-molecular charge transfer from the donor end to the acceptor end of the dye through the conjugated π bridge. The LUMO of a dye is the final state in the charge transition from HOMO to LUMO. Significant contribution of cyanoacrylic acid group (A section) to the LUMO ensures a strong electronic coupling between the dye’s excited state and conduction band of the semiconductor (TiO_2). It facilitates an efficient electron injection as the dye sensitizer is anchored into TiO_2 through the A section. The HOMO is located far away from the A section and therefore TiO_2 surface. Significant contribution of the triphenylamine donor group into the HOMO minimizes the probability of charge recombination between the injected electrons and the resulting oxidized dye [14].

The electron donating substitution ($-\text{NH}_2$) retreats both the HOMO and LUMO of new dye “*ED-I*” from the π -conjugated bridge into the separated D and A sections, respectively, thereby reducing contribution of the R_1 ring of the π -conjugated bridge

in the HOMO, and reducing contribution of the R₂ ring in the D-section of the LUMO of the new dye *ED-I*. On the other hand, the new dye “*EW-I*” with an EW group (-CN) also retreats the HOMO and LUMO of the new dye.

4. Conclusions

The present study aims to enhance appropriate properties such as HOMO-LUMO gap and red-shifting the spectral absorption of an organic dye sensitizer (the TA-St-CA dye) through rational chemical modifications, for the development of new and more efficient organic dye. Perturbational molecular orbital theory (e.g. Dewar’s rule) serves as a good indicator for determination of the appropriate substitution positions on the π -conjugated bridge of the reference dye, and for selection of electron donating/withdrawing building blocks for new dyes. It is found that the electron donating groups (ED substitutions) on position 2* of the reference dye exhibit advantages over the electron withdrawing group (EW substitutes) to reduce the HOMO-LUMO energy gap, as well as to redistribute the electron density of the frontier orbitals (i.e., HOMO and LUMO) of the new dyes. The impact on the optical spectra of new dyes are, however, less significant and warrant further studies in this direction. The rational obtained from present study has been applied to study other dye sensitizers with the D- π -A structures, such as porphyrin derivative dyes which will be presented elsewhere.

Acknowledgements

NM would like to acknowledge Swinburne University Vice-chancellor’s Postgraduate Award. This work is supported by Victorian Partnership for Advanced Computing (VPAC) and Swinburne University Supercomputing Facilities.

References

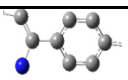
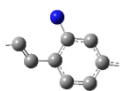
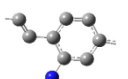
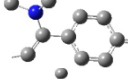
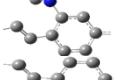
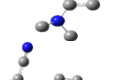
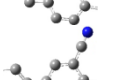
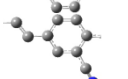
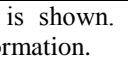
- [1] O'Regan, B., Gratzel, M. A low-cost, high-efficiency solar cell based on dye-sensitized colloidal TiO₂ films. *Nature*. 1991, 353, 737-40.
- [2] Peter, L.M. The Gratzel Cell: Where Next? *J. Phys. Chem. Lett.* . 2011, 2, 1861-7.
- [3] Nazeeruddin, M.K., Kay, A., Rodicio, I., Humphry-Baker, R., Mueller, E., Liska, P., et al. Conversion of light to electricity by cis-X₂bis(2,2'-bipyridyl-4,4'-dicarboxylate)ruthenium(II) charge-transfer sensitizers (X = Cl-, Br-, I-, CN-, and SCN-) on nanocrystalline titanium dioxide electrodes. *J. Am. Chem. Soc.* 1993, 115, 6382-90.
- [4] Grätzel, M. Conversion of sunlight to electric power by nanocrystalline dye-sensitized solar cells. *J. Photochem. Photobiol., A* 2004, 164, 3-14.
- [5] Nazeeruddin, M.K., De Angelis, F., Fantacci, S., Selloni, A., Viscardi, G., Liska, P., et al. Combined Experimental and DFT-TDDFT Computational Study of Photoelectrochemical Cell Ruthenium Sensitizers. *J. Am. Chem. Soc.* 2005, 127, 16835-47.
- [6] Nazeeruddin, M.K., Splivallo, R., Liska, P., Comte, P., Gratzel, M. A swift dye uptake procedure for dye sensitized solar cells. *Chem. Commun.* 2003, 1456-7.
- [7] Péchy, P., Renouard, T., Zakeeruddin, S.M., Humphry-Baker, R., Comte, P., Liska, P., et al. Engineering of Efficient Panchromatic Sensitizers for Nanocrystalline TiO₂-Based Solar Cells. *J. Am. Chem. Soc.* 2001, 123, 1613-24.
- [8] K. Nazeeruddin, M., Pechy, P., Gratzel, M. Efficient panchromatic sensitization of nanocrystalline TiO₂ films by a black dye based on a trithiocyanato-ruthenium complex. *Chem. Commun.* 1997, 1705-6.
- [9] Chiba, Y., Islam, A., Watanabe, Y., Komiya, R., Koide, N., Han, L. Dye-Sensitized Solar Cells with Conversion Efficiency of 11.1%. *Jpn. J. Appl. Phys.*, 45, L638.
- [10] Pastore, M., Mosconi, E., De Angelis, F., Gratzel, M. A Computational Investigation of Organic Dyes for Dye-Sensitized Solar Cells: Benchmark, Strategies, and Open Issues. *J. Phys. Chem. C*. 2010, 114, 7205-12.
- [11] Li, S.-L., Jiang, K.-J., Shao, K.-F., Yang, L.-M. Novel organic dyes for efficient dye-sensitized solar cells. *Chem. Commun.* 2006, 2792-4.
- [12] Heredia, D., Natera, J., Gervaldó, M., Otero, L., Fungo, F., Lin, C.-Y., et al. Spirobifluorene-Bridged Donor/Acceptor Dye for Organic Dye-Sensitized Solar Cells. *Org. Lett.* . 2009, 12, 12-5.
- [13] Hagfeldt, A., Boschloo, G., Sun, L., Kloo, L., Pettersson, H. Dye-Sensitized Solar Cells. *Chem. Rev.* 2010, 110, 6595-663.
- [14] Mishra, A., Fischer, M.K.R., Bäuerle, P. Metal-Free Organic Dyes for Dye-Sensitized Solar Cells: From Structure: Property Relationships to Design Rules. *Angew. Chem., Int. Ed.* 2009, 48, 2474-99.
- [15] Grätzel, M. Dye-sensitized solar cells. *J. Photochem. Photobiol., C* 2003, 4, 145-53.
- [16] Fan, W., Tan, D., Deng, W.-Q. Acene-Modified Triphenylamine Dyes for Dye-Sensitized Solar Cells: A Computational Study. *ChemPhysChem*. 2012, 13, 2051-60.
- [17] Gu, X., Zhou, L., Li, Y., Sun, Q., Jena, P. Design of new metal-free dyes for dye-sensitized solar cells: A first-principles study. *Physics Letters A*. 2012, 376, 2595-9.
- [18] Zhang, J., Kan, Y.-H., Li, H.-B., Geng, Y., Wu, Y., Su, Z.-M. How to design proper π -spacer order of the D- π -A dyes for DSSCs? A density functional response. *Dyes and Pigments*. 2012, 95, 313-21.

- [19] Sanchez-de-Armas, R., San Miguel, M.A., Oviedo, J., Sanz, J.F. Coumarin derivatives for dye sensitized solar cells: a TD-DFT study. *Physical Chemistry Chemical Physics*. 2012, 14, 225-33.
- [20] Sanchez-de-Armas, R., San-Miguel, M.A., Oviedo, J., Sanz, J.F. Molecular modification of coumarin dyes for more efficient dye sensitized solar cells. *The Journal of Chemical Physics*. 2012, 136, 194702-7.
- [21] Yang, L., Guo, L., Chen, Q., Sun, H., Liu, J., Zhang, X., et al. Theoretical design and screening of panchromatic phthalocyanine sensitizers derived from TT1 for dye-sensitized solar cells. *Journal of Molecular Graphics and Modelling*. 2012, 34, 1-9.
- [22] Dewar, M.J.S. 478. Colour and constitution. Part I. Basic dyes. *J. Chem. Soc.* 1950, 2329-34.
- [23] Roughley, S.D., Jordan, A.M. The Medicinal Chemist's Toolbox: An Analysis of Reactions Used in the Pursuit of Drug Candidates. *J. Med. Chem.* . 2011, 54, 3451-79.
- [24] Ooms, F. Molecular Modeling and Computer Aided Drug Design. Examples of their Applications in Medicinal Chemistry. *Curr. Med. Chem.* 2000, 7, 141-58.
- [25] Chen, G.S., Chern, J.-W. Computer-Aided Drug Design. In: *Drug Discovery Research*, John Wiley & Sons, Inc., 2006, pp. 89-107.
- [26] Agrawal, S., English, N.J., Thampi, K.R., Macelroy, J.M. Perspectives on ab initio molecular simulation of excited-state properties of organic dye molecules in dye-sensitized solar cells. *Phys Chem Chem Phys*. 2012, 14, 12044-56.
- [27] Hamann, T.W., Jensen, R.A., Martinson, A.B.F., Van Ryswyk, H., Hupp, J.T. Advancing beyond current generation dye-sensitized solar cells. *Energy & Environmental Science*. 2008, 1, 66-78.
- [28] Martsinovich, N., Troisi, A. Theoretical studies of dye-sensitized solar cells: from electronic structure to elementary processes. *Energy & Environmental Science*. 2011, 4, 4473-95.
- [29] Zhang, J., Li, H.-B., Sun, S.-L., Geng, Y., Wu, Y., Su, Z.-M. Density functional theory characterization and design of high-performance diarylamine-fluorene dyes with different [small pi] spacers for dye-sensitized solar cells. *Journal of Materials Chemistry*. 2012, 22, 568-76.
- [30] Geiger, T., Kuster, S., Yum, J.-H., Moon, S.-J., Nazeeruddin, M.K., Grätzel, M., et al. Molecular Design of Unsymmetrical Squaraine Dyes for High Efficiency Conversion of Low Energy Photons into Electrons Using TiO₂ Nanocrystalline Films. *Adv. Funct. Mater.* 2009, 19, 2720-7.
- [31] Hung, J., Liang, W., Luo, J., Shi, Z., Jen, A.K.Y., Li, X. Rational Design Using Dewar's Rules for Enhancing the First Hyperpolarizability of Nonlinear Optical Chromophores. *J. Phys. Chem. C*. 2010, 114, 22284-8.
- [32] Hwang, S., Lee, J.H., Park, C., Lee, H., Kim, C., Park, C., et al. A highly efficient organic sensitizer for dye-sensitized solar cells. *Chem. Commun.* . 2007, 4887-9.
- [33] Adamo, C., Barone, V. Toward reliable density functional methods without adjustable parameters: The PBE0 model. *Chin. J. Chem. Phys.* 1999, 110, 6158-70.
- [34] Tao, J., Tretiak, S., Zhu, J.-X. Absorption Spectra of Blue-Light-Emitting Oligoquinolines from Time-Dependent Density Functional Theory. *J. Phys. Chem. B*. 2008, 112, 13701-10.
- [35] Adamo, C., Barone, V. Accurate excitation energies from time-dependent density functional theory: assessing the PBE0 model for organic free radicals. *Chem. Phys. Lett.* 1999, 314, 152-7.

- [36] Jacquemin, D., Perpète, E.A., Scuseria, G.E., Ciofini, I., Adamo, C. TD-DFT Performance for the Visible Absorption Spectra of Organic Dyes: Conventional versus Long-Range Hybrids. *J. Chem. Theory Comput.* 2007, 4, 123-35.
- [37] Gaussian 09, M.J.F., G. W. Trucks, H. B. Schlegel, G. E. Scuseria, M. A. Robb, J. R. Cheeseman, G. Scalmani, V. Barone, B. Mennucci, G. A. Petersson, H. Nakatsuji, M. Caricato, X. Li, H. P. Hratchian, A. F. Izmaylov, J. Bloino, G. Zheng, J. L. Sonnenberg, M. Hada, M. Ehara, K. Toyota, R. Fukuda, J. Hasegawa, M. Ishida, T. Nakajima, Y. Honda, O. Kitao, H. Nakai, T. Vreven, J. A. Montgomery, Jr., J. E. Peralta, F. Ogliaro, M. Bearpark, J. J. Heyd, E. Brothers, K. N. Kudin, V. N. Staroverov, R. Kobayashi, J. Normand, K. Raghavachari, A. Rendell, J. C. Burant, S. S. Iyengar, J. Tomasi, M. Cossi, N. Rega, J. M. Millam, M. Klene, J. E. Knox, J. B. Cross, V. Bakken, C. Adamo, J. Jaramillo, R. Gomperts, R. E. Stratmann, O. Yazyev, A. J. Austin, R. Cammi, C. Pomelli, J. W. Ochterski, R. L. Martin, K. Morokuma, V. G. Zakrzewski, G. A. Voth, P. Salvador, J. J. Dannenberg, S. Dapprich, A. D. Daniels, Ö. Farkas, J. B. Foresman, J. V. Ortiz, J. Cioslowski, and D. J. Fox, Gaussian, Inc., Wallingford CT. 2009.
- [38] Selvam, L., Vasilyev, V., Wang, F. Methylation of Zebularine: A Quantum Mechanical Study Incorporating Interactive 3D pdf Graphs. *The Journal of Physical Chemistry B.* 2009, 113, 11496-504.
- [39] Cossi, M., Rega, N., Scalmani, G., Barone, V. Energies, structures, and electronic properties of molecules in solution with the C-PCM solvation model. *J Comput Chem.* 2003, 24, 669-81.
- [40] Barone, V., Cossi, M. Quantum calculation of molecular energies and energy gradients in solution by a conductor solvent model. *J Phys Chem A.* 1998, 102, 1995-2001.
- [41] Ganesan, A., Wang, F., Falzon, C. Intramolecular interactions of L-phenylalanine: Valence ionization spectra and orbital momentum distributions of its fragment molecules. *J. Comput. Chem.* 2011, 32, 525-35.
- [42] Zhang, C.-R., Liu, Z.-J., Chen, Y.-H., Chen, H.-S., Wu, Y.-Z., Feng, W., et al. DFT and TD-DFT study on structure and properties of organic dye sensitizer TA-St-CA. *Curr. Appl. Phys.* 2010, 10, 77-83.
- [43] Persson, P., Lundqvist, M.J. Calculated Structural and Electronic Interactions of the Ruthenium Dye N3 with a Titanium Dioxide Nanocrystal. *The Journal of Physical Chemistry B.* 2005, 109, 11918-24.
- [44] De Angelis, F. Direct vs. indirect injection mechanisms in perylene dye-sensitized solar cells: A DFT/TDDFT investigation. *Chem Phys Lett.* 2010, 493, 323-7.
- [45] Agrawal, S., Dev, P., English, N.J., Thampi, K.R., MacElroy, J.M.D. A TD-DFT study of the effects of structural variations on the photochemistry of polyene dyes. *Chemical Science.* 2012, 3, 416-24.
- [46] Fan, W., Tan, D., Deng, W. Theoretical investigation of triphenylamine dye/titanium dioxide interface for dye-sensitized solar cells. *Physical Chemistry Chemical Physics.* 2011, 13, 16159-67.
- [47] Agrawal, S., Dev, P., English, N.J., Thampi, K.R., MacElroy, J.M.D. First-principles study of the excited-state properties of coumarin-derived dyes in dye-sensitized solar cells. *Journal of Materials Chemistry.* 2011, 21, 11101-8.
- [48] De Angelis, F., Fantacci, S., Selloni, A., Grätzel, M., Nazeeruddin, M.K. Influence of the Sensitizer Adsorption Mode on the Open-Circuit Potential of Dye-Sensitized Solar Cells. *Nano Letters.* 2007, 7, 3189-95.

- - , J., A. San-Miguel, M., Sanz
, P., Pruneda, M. Real-Time TD-DFT Simulations in Dye Sensitized Solar Cells: The Electronic Absorption Spectrum of Alizarin Supported on TiO₂ Nanoclusters. *Journal of Chemical Theory and Computation*. 2010, 6, 2856-65.
- [50] Wen, P., Han, Y., Zhao, W. Influence of TiO₂ Nanocrystals Fabricating Dye-Sensitized Solar Cell on the Absorption Spectra of N719 Sensitizer. *International Journal of Photoenergy*. 2012, 2012, 7.
- [51] Duncan, W.R., Prezhdo, O.V. Theoretical studies of photoinduced electron transfer in dye-sensitized TiO₂. *Annu Rev Phys Chem*. 2007, 58, 143-84.
- [52] Jaffe, H.H. The molecular orbital theory of organic chemistry (Dewar, Michael J. S.). *J. Chem. Educ.* 1970, 47, A531.
- [53] Huang, F., Li, Q., Thorogood, G.J., Cheng, Y.-B., Caruso, R.A. Zn-doped TiO₂ electrodes in dye-sensitized solar cells for enhanced photocurrent. *Journal of Materials Chemistry*. 2012, 22, 17128-32.

Table 1: Pictorial list of substitutions on π bridge (Hydrogens are not display

Substitution Name(Label)	Picture ^(a)	Substitution Type	Substitution Group	Position
ED-I		Electron Donating	NH ₂	2*
ED-II				4*
ED-III				8*
ED-IV			N(CH ₃) ₂	2*
ED-V				4*
ED-VI				8*
EW-I		Electron Withdrawing	CN	1
EW-II				5
EW-III				7

a. Only π bridge is shown. For complete structures refer to Table S1 in supplementary information.

Table 2: π -length (in Å) and dipole moment (in Debye) of TA-ST-CA dye and its modifications*.

	TA-St-CA	ED-I ^(a)	ED-II ^(a)	ED-III ^(a)	ED-IV ^(a)	ED-V ^(a)	ED-VI ^(a)	EW-I ^(a)	EW-II ^(a)	EW-III ^(a)
π -length ^(b) (Å)	5.23	5.13	5.19	5.26	5.10	5.20	5.27	5.33	5.24	5.23
$\langle R^2 \rangle$ (a.u)	34612.20	34474.2	35088.40	35182.90	35646.00	36605.00	36285.80	35192.60	36808.20	36088.30
μ (Debye)	6.58	4.63	5.82	6.82	4.64	5.68	6.55	8.38	8.41	8.81

Optimized at PBE0/6-31G level.

(a) Refer to Table 1 for labels.

(b) Direct distance of C₁₈-C₂₃.

Table 3: Comparison of the substitution effects on the energies of the HOMOs (ϵ_{HOMO}), the LUMOs (ϵ_{LUMO}), the HOMO-LUMO energy gap ($\Delta\epsilon$), shift of the spectral peaks ($\Delta\lambda_{\text{I}}$ and $\Delta\lambda_{\text{II}}$) and spectral widths ($\Delta\gamma_{\text{I}}$ and $\Delta\gamma_{\text{II}}$) in ethanol solution*.

Dyes	$\Delta\epsilon$ ^(a)	ϵ_{HOMO} ^(b)	ϵ_{LUMO} ^(c)	$\Delta(\Delta\epsilon)$ ^(d)	$\Delta\lambda_{\text{I}}$ (360 nm) ^(e)	$\Delta\lambda_{\text{II}}$ (500 nm) ^(e)	$\Delta\gamma_{\text{I}}$ (360 nm) ^(f)	$\Delta\gamma_{\text{II}}$ (500 nm) ^(f)
TA-St-CA	2.68	NA ^(g)	NA ^(g)	NA ^(g)	NA ^(g)	NA ^(g)	NA ^(g)	NA ^(g)
ED-I ^(h)	2.53	+	+	—	—	+	+	—
ED-II ^(h)	2.70	+	+	+	—	NC ⁽ⁱ⁾	—	+
ED-III ^(h)	2.66	+	+	—	—	+	—	+
ED-IV ^(h)	2.49	+	+	—	—	+	+	—
ED-V ^(h)	2.67	+	+	—	—	+	—	+
ED-VI ^(h)	2.63	+	+	—	—	+	NC ⁽ⁱ⁾	NC ⁽ⁱ⁾
EW-I ^(h)	2.51	—	—	—	+	+	+	—
EW-II ^(h)	2.40	—	—	—	+	+	+	—
ED-III ^(h)	2.60	—	—	—	+	+	+	—

* Black indicates the preferred shift and red indicates the unwanted changes.

(a) HOMO-LUMO gap (eV).

(b) Indicates whether HOMO level is shifted up (+) or down (—) compared to TA-St-CA base structure.

(c) Indicates whether LUMO level is shifted up (+) or down (—) compared to TA-St-CA base structure.

(d) Indicates whether HOMO-LUMO gap is decreased (—) or increased (+) compared to TA-St-CA base structure.

(e) Indicates a bathochromic shift (+) or hypsochromic shift (—) of this peak compared to TA-St-CA base structure.

(f) Indicates an increase of peak width (+) or a decrease of peak width (—) of this peak compared to TA-St-CA base structure.

(g) NA=Not applicable.

(h) Refer to Table 1 for labels.

(i) NC= Not changed.

Figure Captions

Figure 1. The structure of reference dye TA-St-CA. Atoms on conjugated bridge (indicated by brackets) are marked alternatively by asterisks. Note that structure is saturated by hydrogen atoms which are not displayed on the structure. Double click on the TA-St-CA dye structure will activate the 3D-pdf function. Use the mouse to move the structure for a better view of the structure in 3D space.

Figure 2. The simulated UV–Vis absorption spectra of TA-ST-CA dye and its substituted new dyes “*ED-I to EW-III*” in ethanol using the TD-DFT calculations. Refer to Table 1 for new dyes labels and structures.

Figure 3. Calculated frontier MO energy levels using PBE0/6-31G* in vacuum. Refer to Table 1 for the new dye labels and structures.

Figure 4. Comparison of the HOMOs (left) and LUMOs (right) of the new dye, *ED-I* and *EW-I* with respect to those of the reference TA-St-CA dye.

Fig.1

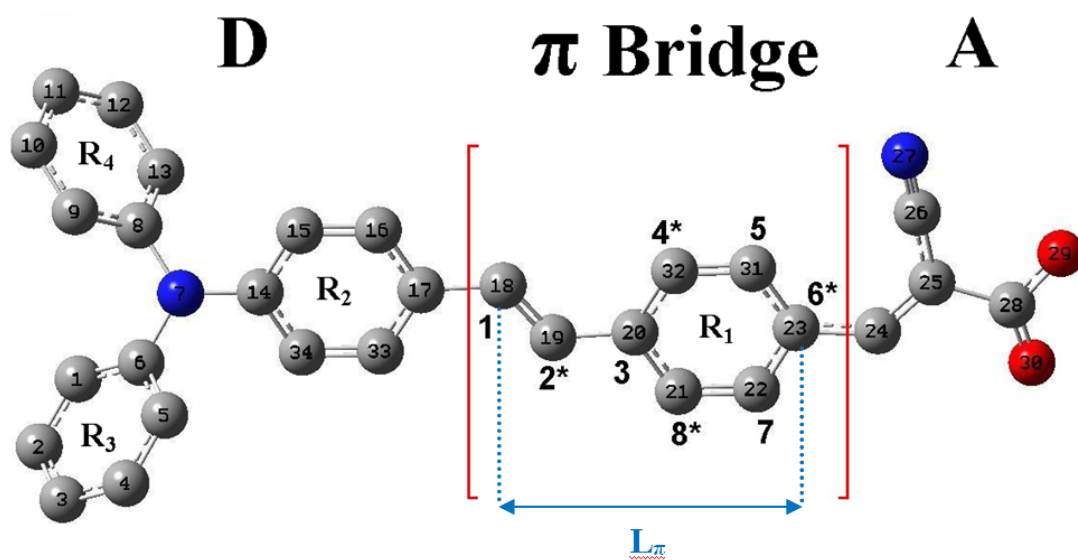


Fig.2

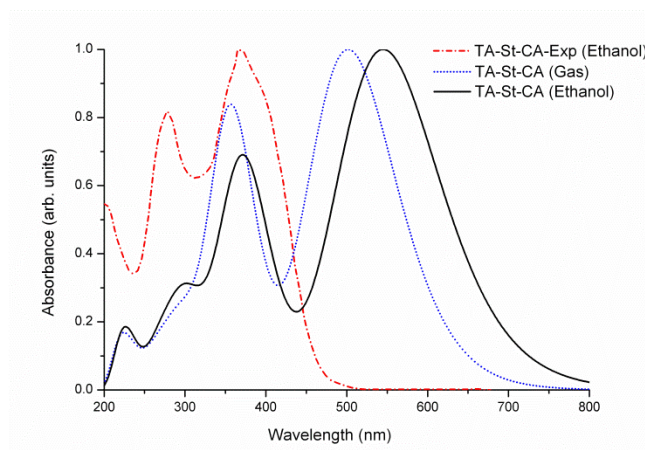
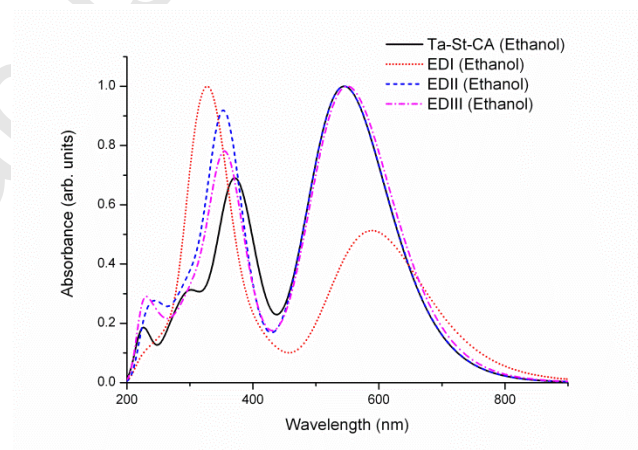
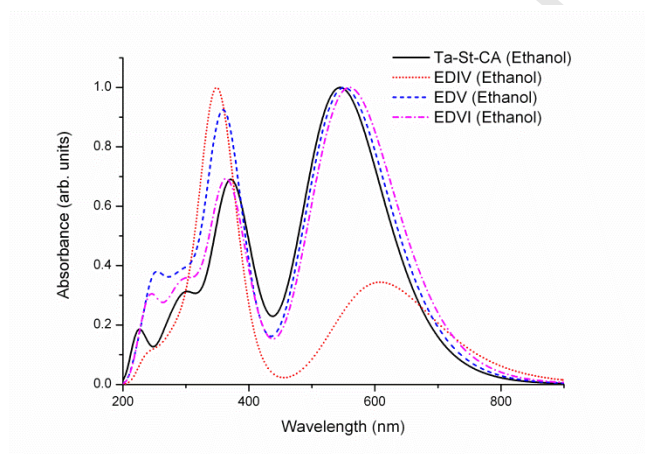
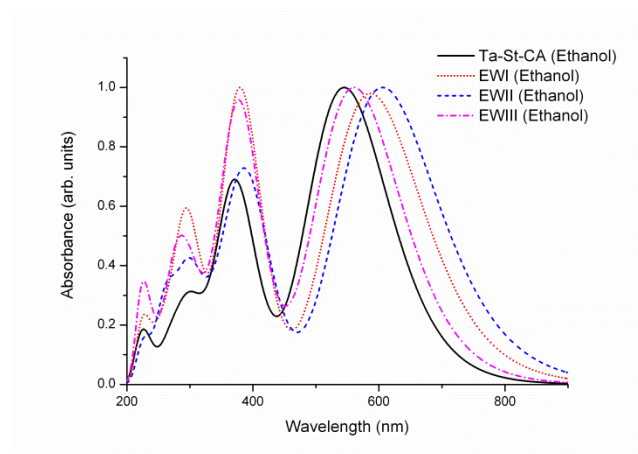
**a₁****a₂****a₃****a₄**

Fig.3

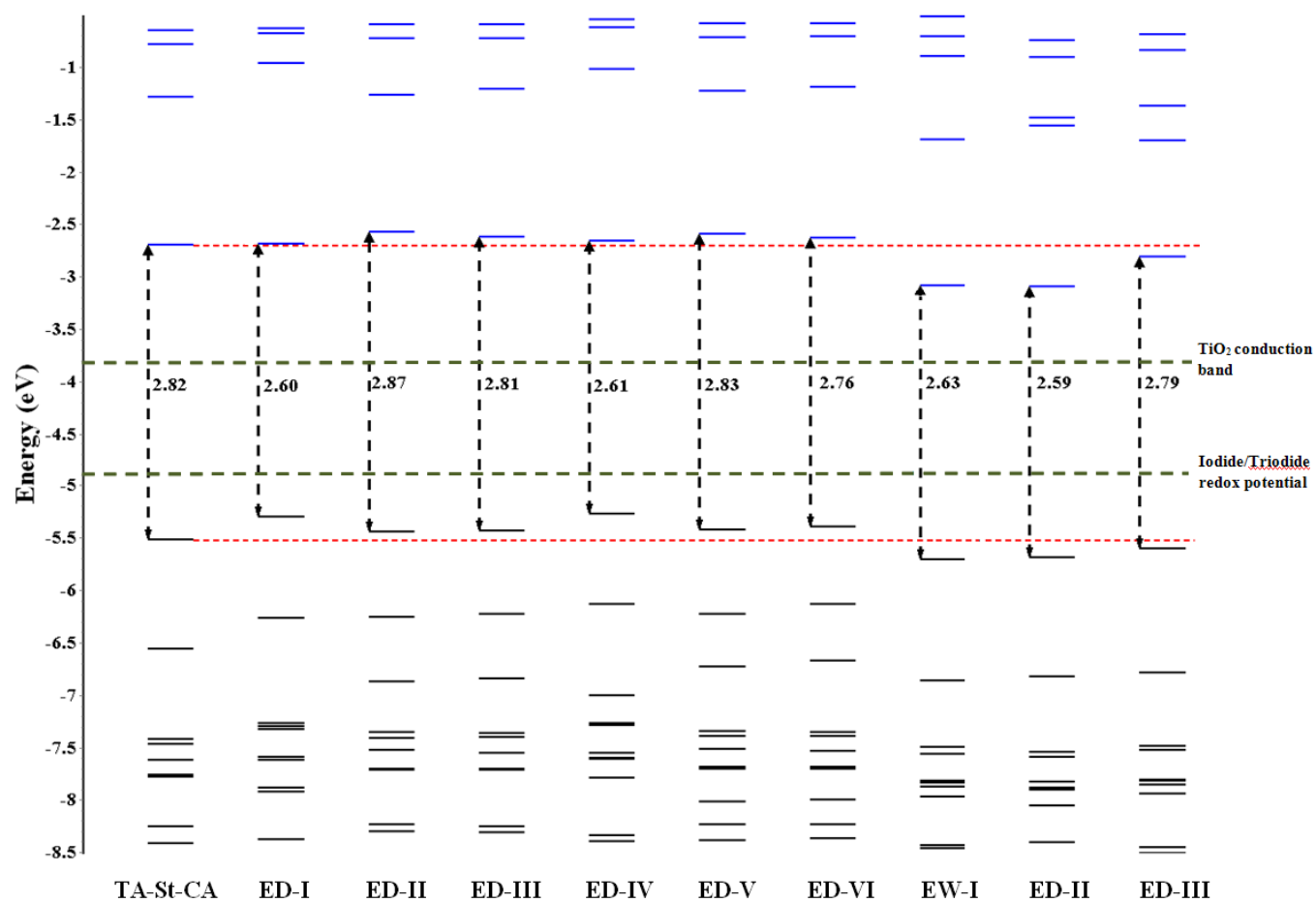


Fig. 4

